Theory of damped Bloch waves in elastic media

Mahmoud I. Hussein*
Department of Aerospace Engineering Sciences, University of Colorado at Boulder, Boulder, Colorado 80309-0429, USA
(Received 14 October 2009; published 2 December 2009)

We present a theory for Bloch wave propagation in damped elastic media. We expand the eigenvalue problem governing the dispersion relation using a set of Bloch mode eigenvectors at each wave-vector point. With the assumption of Rayleigh damping, this decomposition allows us to derive the band structure in the Brillouin zone. The damping ratio corresponding to each Bloch mode is also generated. We show that damping qualitatively alters the shape of the dispersion curves. Damping also results in a branch-overtaking phenomenon that has a significant effect on band gaps. As the damping is increased, a band-gap size can drop abruptly.

DOI: 10.1103/PhysRevB.80.212301 PACS number(s): 62.30.+d, 62.65.+k, 63.20.−e

Periodic elastic materials, such as phononic crystals, can be designed, via band engineering, to classically control the propagation of sound and/or elastic waves in a predetermined manner within solids, or within solid-fluid systems. In doing so, these modern materials have opened up a technological frontier in acoustic and elastic devices.[1,2] In many cases, one or more of the constituent materials are damped (i.e., dissipative), a good example is viscoelastic materials which are often used to form the matrix phase in phononic crystal composites. Another example is the presence of damping in the supports of periodic engineering structures.[3] The presence of damping results in temporal attenuation of the elastic waves as they freely "progress" through the periodic media.[3] Such damped free wave-propagation characteristics can be of high importance if, for example, a structure composed of a viscoelastic phononic crystal is subjected to continuous forcing (i.e., a sustained source of energy input). The short-timed response to a shock load is also influenced by the level of damping. Mead[3] presented an early study of damping in infinite periodic structures. Focusing on one-dimensional (1D) discrete mass-spring models, he dealt with structural (velocity independent) damping as well as with a hypothetical type of damping associated with what was referred to as "damped forced modes." Viscous damping was treated later on with various types of dissipative constitutive models. Mukherjee and Lee[4] provided a 1D dispersion relation using a complex elastic modulus to model viscoelasticity. However, no wave-number-dependent relation was available for the damping. In other studies, often the focus has been on finite structures or there was little consideration of the broad effects on the band-structure characteristics (e.g., Refs. 5 and 6). Some studies explicitly investigated the band structure but only using viscoelastic damping models that were either limited to a fixed frequency[7,8] or to low frequencies.[9] Wang *et al.*[10] analytically studied dispersion in 1D viscoelastic lattices with a valid frequency-dependent model. Merheb *et al.*[11] also provided a study that was not limited to certain frequencies, using the finite-difference time-domain method in addition to experiments. Yet both these studies did not provide a detailed analysis of the broad effects of damping on the dispersion band structure. In Ref. 11, the conclusions were focused on the attenuation/decay effects.

In this paper, we provide a theory for analyzing frequency-dependent viscously damped periodic media and give a detailed analysis on the effects of damping on the frequency band structure, and associated phase and group-velocity dispersion curves. We consider continuous media governed by $\nabla\cdot\boldsymbol{\sigma}=\rho\ddot{\mathbf{u}}$, where $\boldsymbol{\sigma}$ is the stress tensor, $\mathbf{u}$ is the displacement field, ρ is the density, and a superposed dot denotes differentiation with respect to time. The constitutive behavior is treated phenomenologically assuming linear and isotropic elastic response and Rayleigh-type damping. A Rayleigh damping model assumes that the viscous damping operator in the governing equation is proportional to the mass and stiffness operators with predetermined constants of proportionality, $\bar{p}$ and $\bar{q}$, respectively.[12] The material-to-material interfaces are assumed to be ideal. Upon spatial discretization, for example, using the finite element method, and assuming no external forcing, the following matrix equation is obtained:

$$\mathbf{M}\ddot{\mathbf{U}}+\mathbf{C}\dot{\mathbf{U}}+\mathbf{K}\mathbf{U}=\mathbf{0}, \tag{1}$$

where $\mathbf{U}$ is the displacement vector and $\mathbf{M}$, $\mathbf{C}$, and $\mathbf{K}$ denote the mass, damping, and stiffness matrices, respectively. Following the Rayleigh model, the $\mathbf{C}$ matrix has the form $\mathbf{C}=\bar{p}\mathbf{M}+\bar{q}\mathbf{K}$.

Applying Bloch theory on a unit cell yields a free plane-wave solution of the form

$$\mathbf{U}(\mathbf{x},\mathbf{k};t)=\tilde{\mathbf{U}}(\mathbf{x},\mathbf{k})e^{i(\mathbf{k}^T\mathbf{x}-\omega t)}, \tag{2}$$

where $\mathbf{x}=\{x,y,z\}$ is the position vector, $\mathbf{k}=\{k_x,k_y,k_z\}$ is the wave vector, $i=\sqrt{-1}$, and ω and t denote frequency and time, respectively. In Eq. (2), $\tilde{\mathbf{U}}$ is the displacement Bloch vector which is periodic within the unit-cell domain. Using Eq. (2), the following Bloch matrix equation is obtained

$$-\omega^2\mathbf{M}\tilde{\mathbf{U}}-i\omega\mathbf{C}(\mathbf{k})\tilde{\mathbf{U}}+\mathbf{K}(\mathbf{k})\tilde{\mathbf{U}}=\mathbf{0}. \tag{3}$$

The presence of the second term in the left-hand side of Eq. (3) prevents us from generating an eigenvalue problem in the usual way for calculating the band structure. We therefore employ the concept of *Bloch mode expansion*[13] which allows us to linearly transform the model to a set of generalized coordinates, $\tilde{\mathbf{V}}$, i.e.,

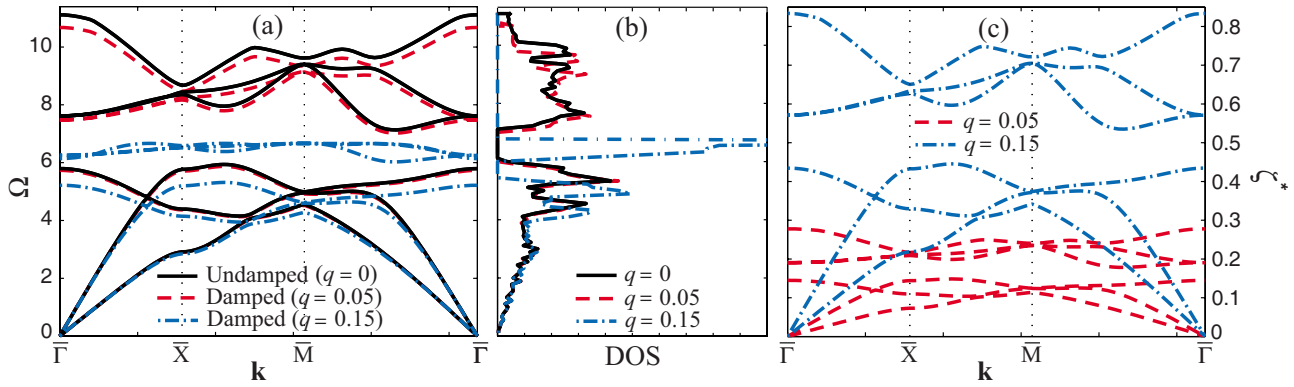

FIG. 1. (Color online) (a) Frequency band structure, (b) density of states, and (c) damping-ratio band structure for undamped ($q=0$) and damped ($q=0.05$ and $q=0.15$) phononic crystals.

$$\tilde{\mathbf{U}}_{(n\times 1)} = \boldsymbol{\Psi}(\mathbf{k})_{(n\times m)}\tilde{\mathbf{V}}_{(m\times 1)}, \tag{4}$$

where $\boldsymbol{\Psi}(\mathbf{k})$ is a Bloch modal matrix. In Eq. (4), n and m, respectively, denote the total number of degrees of freedom and the total number of Bloch modes retained in the expansion. Unlike in Ref. 13 in which the aim was model reduction, here the matrix $\boldsymbol{\Psi}(\mathbf{k})$ is formed using a set of Bloch vectors obtained by solving the standard undamped eigenvalue problem [Eq. (3) with $\mathbf{C}=\mathbf{0}$] at the *current* point $\mathbf{k}$ in the reciprocal-lattice space.[14] Utilizing the orthogonality condition that the Bloch vectors exhibit with respect to $\mathbf{M}$ and $\mathbf{K}$, we use this expansion to uncouple the equations in Eq. (3). This is done by substituting Eq. (4) into Eq. (3) and premultiplying all terms by $\boldsymbol{\Psi}^*$, where the asterisk denotes the complex transpose operation. Returning to Eq. (4), only as many Bloch modes, m, need to be incorporated in the expansion as the number of branches of interest in the damped band diagram that is to be generated. The result is a set of m uncoupled equations $-\omega^2\tilde{V}_j - i\omega 2\zeta_j^*(\mathbf{k})\omega_j(\mathbf{k})\tilde{V}_j + \lambda_j(\mathbf{k})\tilde{V}_j = 0$, $j=1,\ldots,m$, where $\tilde{V}_j$ is the jth generalized coordinate, $\lambda_j(\mathbf{k})$ is the eigenvalue of the jth branch of the undamped band structure at point $\mathbf{k}$ and $\omega_j(\mathbf{k})$ is the frequency, i.e., $\omega_j(\mathbf{k})=\sqrt{\lambda_j(\mathbf{k})}$. Of special interest now is $\zeta_j^*(\mathbf{k})$, which is the damping ratio of the jth branch of the damped band structure at point $\mathbf{k}$ and has the form

$$\zeta_j^*(\mathbf{k}) = \frac{\bar{p} + \bar{q}\lambda_j(\mathbf{k})}{2\omega_j(\mathbf{k})}. \tag{5}$$

We can now write the Bloch solution in generalized coordinates as $V_j = \tilde{V}_j e^{i(\mathbf{k}^T\mathbf{x}-\omega t)}$. From this solution and its time derivatives, we can extract the following ordinary differential equation describing the temporal response V_j corresponding to each of the generalized coordinates

$$\ddot{V}_j + 2\zeta_j^*(\mathbf{k})\omega_j(\mathbf{k})\dot{V}_j + \lambda_j(\mathbf{k})V_j = 0, \quad j=1,\ldots,m. \tag{6}$$

Equation (6) can be solved by assuming a position- and wave-vector-dependent harmonic solution in time, $V_j = A_j(\mathbf{x},\mathbf{k})e^{\alpha_j(\mathbf{k})t}$, where $A_j(\mathbf{x},\mathbf{k}) = \tilde{V}_j e^{i\mathbf{k}^T\mathbf{x}}$ denotes amplitude of oscillation, yielding the following expression for the roots: $\alpha_j(\mathbf{k}) = -\zeta_j^*(\mathbf{k})\omega_j \pm \omega_j\sqrt{\zeta_j^*(\mathbf{k})^2 - 1}$. For the undamped case $[\zeta_j^*(\mathbf{k})=0]$, the frequency of the jth branch of the original undamped band structure is recovered. For $\zeta_j^*(\mathbf{k})<1$, the medium is underdamped at $\mathbf{k}$ and propagating waves exhibit temporal decay. Subsequently the wave-vector-dependent *frequency of damped oscillation* can be identified as

$$\omega_{d_j}(\mathbf{k}) = \omega_j(\mathbf{k})\sqrt{1-\zeta_j^*(\mathbf{k})}, \tag{7}$$

which is essentially the frequency of the jth branch of the damped band structure at point $\mathbf{k}$. For $\zeta_j^*(\mathbf{k})>1$, the medium is overdamped at $\mathbf{k}$ and temporal oscillations cannot exist. The medium is critically damped at $\mathbf{k}$ when $\zeta_j^*(\mathbf{k})=1$. It is noteworthy that this theory is analogous to the well-established modal-decomposition theory for proportionally damped *finite* structures.[15]

We now examine the behavior of proportionally damped periodic media such as phononic crystals. We use the finite element method to first solve Eq. (3) with $\mathbf{C}=\mathbf{0}$, then proceed to calculating $\zeta_j^*(\mathbf{k})$ and $\omega_{d_j}(\mathbf{k})$ by simply post-processing the resulting undamped band-structure data using Eqs. (5) and (7), respectively. The above formulation is applicable to three-dimensional models. However, for ease of exposition we present results for a two-dimensional model under plane strain conditions. In our example model, a square lattice is considered with a bi-material unit cell consisting of a centrally located square inclusion. The filling ratio is 0.3086. The material phase for the matrix (denoted by subscript "1") is chosen to be compliant and light while the phase for the inclusion (denoted by subscript "2") is stiff and dense. In particular, a ratio of Young's moduli of $E_2/E_1=20$ and a ratio of densities of $\rho_2/\rho_1=2$ are chosen. A Poisson ratio of 0.34 is assumed for both phases. The unit-cell finite-element mesh consists of 18×18 uniformly sized four-node bilinear quadrilateral elements. The path along the symmetry points, $\bar{\Gamma}\to\bar{\mathrm{X}}\to\bar{\mathrm{M}}\to\bar{\Gamma}$, bordering the irreducible Brillouin zone is sampled into ninety seven $\mathbf{k}$-point steps. In the results, we refer to the degree of damping using the scaled parameters p and q, defined as $p=\bar{p}\sqrt{\mu_1/\rho_1}/a$ and $q=\bar{q}a/\sqrt{\mu_1/\rho_1}$, respectively, were a denotes the unit-cell side length (set to unity) and μ_1 denote the shear Lamé constant for material phase 1.

Figure 1 shows the band structure and density of states for the undamped case, where $q=0$, and for two damped cases corresponding to $q=0.05$ and $q=0.15$. The frequency is de-

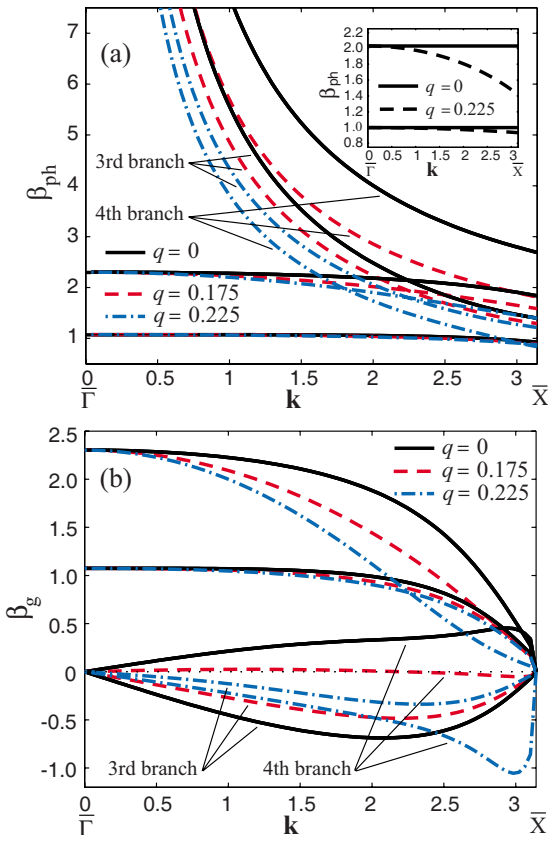

FIG. 2. (Color online) (a) Phase and (b) group-velocity dispersion curves for undamped (q=0) and damped (q=0.175 and q=0.225) phononic crystals along the $\bar{\Gamma}\rightarrow\bar{\mathrm{X}}$ path. The inset in (a) shows the dispersion curves for an undamped (q=0) and a damped (q=0.225) homogenous material.

fined as $\Omega=\omega_d a/\sqrt{\mu_1/\rho_1}$. The damping ratio corresponding to each mode at each branch, as a function of $\mathbf{k}$, is also shown. We see that the location of the branches in the frequency domain drop with damping and do so at an increasing rate as the damping ratio increases. The damping ratio band structure resembles the frequency band structure in shape with the locations of the curves rising with increase in q. We also studied the case where $p\neq 0$ and q=0 (not shown). Here, the frequency band structure away from the $\bar{\Gamma}$ point experiences very small shifts whereas at and near the $\bar{\Gamma}$ point the downward shift in frequencies is dramatic and this is due to sharp increases in ζ_j^* within this neighborhood. In fact with a small increase in p, the value of the damping ratio at and near the $\bar{\Gamma}$ point exceeds unity, i.e., exceeds the critical damping level beyond which there is no temporal oscillations. We therefore focus on varying q while keeping p=0. Figure 2 shows the phase and group-velocity dispersion curves in the $\bar{\Gamma}\rightarrow\bar{\mathrm{X}}$ segment. We note that the group velocity changes from positive to negative as a result of damping for some branches, e.g., the fourth branch. The shapes of the group-velocity curves are also dramatically altered as damping is increased, especially the higher branches. These damping-related dispersive effects bear significant consequences as the direction and manner by which information

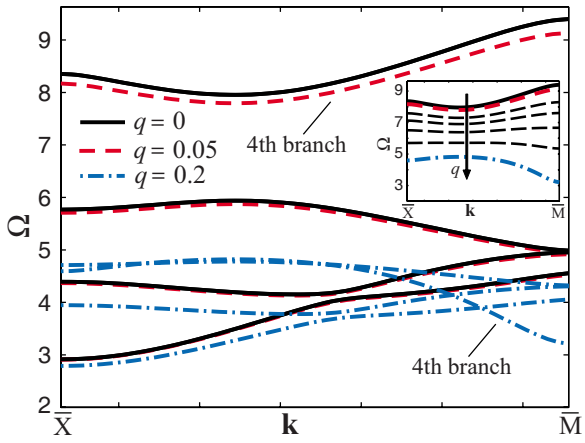

FIG. 3. (Color online) A focus on the band structure along the $\bar{\mathrm{X}}\rightarrow\bar{\mathrm{M}}$ path for undamped (q=0) and damped (q=0.05 and q=0.2) phononic crystals, demonstrating the phenomenon of branch overtaking. The inset shows the downward progression, and change of trend, of the fourth branch as the damping parameter q is gradually increased.

and energy flow are altered. It is noteworthy that damping is shown to transform a nondispersive homogeneous medium to one that is dispersive [as illustrated in the inset of Fig. 2(a)]. In Fig. 3 we focus on the $\bar{\mathrm{X}}\rightarrow\bar{\mathrm{M}}$ segment to highlight that with sufficient damping, higher branches drop at rates higher than lower branches thus enabling *branch overtaking*. We observe that the fourth branch completely overtakes the third in its downward shift as q is increased. It also surpasses the second and first branches near the M point. This remarkable branch-overtaking phenomenon is also evident in the velocity dispersion curves in Fig. 2. This phenomenon is

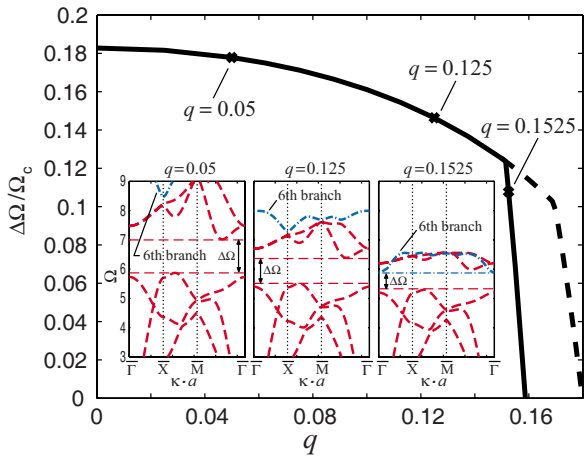

FIG. 4. (Color online) Relative size of band gap as a function of Rayleigh damping parameter q. An abrupt drop is observed at $q\approx$0.15 due to the branch-overtaking phenomenon brought about by the presence of viscous damping. The insets monitor the progression of the sixth branch as the damping is increased. At q=01525, this branch has lower values than the fourth branch near the $\bar{\Gamma}$ point leading to an abrupt drop in the band-gap size. The dashed line in the main plot projects the original reduction in $\Delta\Omega/\Omega_C$ until the next overtaking in which the seventh branch surpasses the fourth.

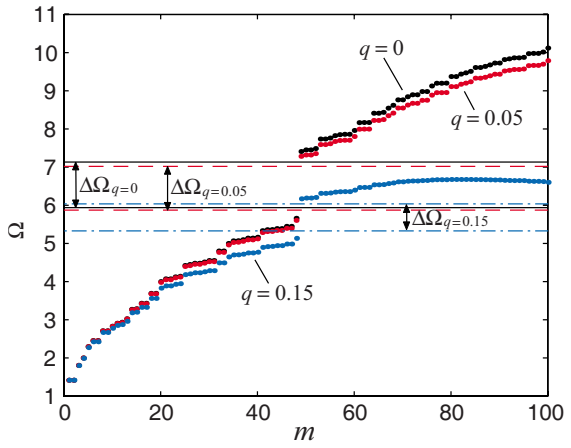

FIG. 5. (Color online) Vibration natural frequency as a function of mode number m for finite 4×4 unit cell phononic crystal with the same parameters as the infinite case. Results are shown for the undamped case ($q=0$) and the same damped cases as in Fig. 1 ($q=0.05$ and $q=0.15$). The horizontal lines indicate the band-gap locations based on the infinite phononic crystal band structure.

particularly important when considering band gaps and their dependency on damping. From Fig. 1, we note that the unit cell considered exhibits a band gap between the third and fourth branches, in its undamped form. Figure 4 presents the relative size of this band gap (width $\Delta\Omega$ divided by central frequency Ω_c) as a function of q. We observe clearly an *abrupt drop* in the band-gap size and this is due to the fast-falling sixth branch overtaking the fourth when the level of damping reaches $q\approx0.15$. Viscous damping induces phase changes which cause the observed shifts in the frequencies. However with these shifts, each Bloch mode along each branch still retains its character (i.e., mode shape) even when branch overtaking occurs. Finally, we look at a finite structure composed of an array of the same unit cell studied in order to confirm the validity of our damped band-structure theory and all the previous results. The finite structure we consider consists of 4×4 cells and is fixed at all edges and corners. Using the same finite-element model parameters as for the Bloch unit-cell analysis, we calculate the natural frequencies for the undamped and damped cases considered in Fig. 1. We find from the results, presented in Fig. 5, that the "gaps" in the finite-structure natural frequencies correlate perfectly with the band gaps marked in Fig. 1 for the infinite structure. This is a key comparison considering that the calculation of natural frequencies of finite structures is well established.[15] These results therefore support the validity of our theory. Conversely, the Bloch unit cell analysis results explain why natural frequency gaps in finite periodic structures alter abruptly with damping. While we focused on phononic crystals, the presented Bloch modal analysis theory is also relevant to the study of dissipation in other types of periodic media such as photonic crystals.[16]

*mih@colorado.edu

[1] M. S. Kushwaha, P. Halevi, L. Dobrzynski, and B. Djafari-Rouhani, Phys. Rev. Lett. **71**, 2022 (1993).
[2] M. Sigalas, M. S. Kushwaha, E. N. Economou, M. Kafesaki, I. E. Psarobas, and W. Steurer, Z. Kristallogr. **220**, 765 (2005).
[3] D. J. Mead, J. Sound Vib. **27**, 235 (1973).
[4] S. Mukherjee and E. H. Lee, Comput. Struct. **5**, 279 (1975).
[5] I. E. Psarobas, Phys. Rev. B **64**, 012303 (2001).
[6] P. W. Mauriz, M. S. Vasconcelos, and E. L. Albuquerque, Phys. Status Solidi B **243**, 1205 (2006).
[7] R. Sprik and G. H. Wegdam, Solid State Commun. **106**, 77 (1998).
[8] X. Zhang, Z. Liu, J. Mei, and Y. Liu, J. Phys.: Condens. Matter **15**, 8207 (2003).
[9] Y. Liu, D. Yu, H. Zhao, J. Wen, and X. Wen, J. Phys. D **41**, 065503 (2008).
[10] W. Wang, J. Yu, and Z. Tang, Phys. Lett. A **373**, 5 (2008).
[11] B. Merheb, P. A. Deymier, M. Jain, M. Aloshyna-Lesuffleur, S. Mohanty, A. Baker, and R. W. Greger, J. Appl. Phys. **104**, 064913 (2008).
[12] T. K. Caughey and M. E. J. O'Kelly, ASME J. Appl. Mech. **32**, 583 (1965).
[13] M. I. Hussein, Proc. R. Soc. London, Ser. A **465**, 2825 (2009).
[14] A "**k** point" designates a particular wave vector in the reciprocal-lattice space of the unit cell.
[15] L. Meirovitch, *Principles and techniques of vibrations* (Prentice-Hall, London, UK, 1997).
[16] V. Kuzmiak and A. A. Maradudin, Phys. Rev. B **58**, 7230 (1998).